JOURNAL OF APPLIED ELECTROCHEMISTRY 26 (1996) 617–622

Electrochemically induced alumina coatings on stainless steel: composition and behaviour at high temperature

L. ARIES, J. ROY, J. SOTOUL, V. PONTET

Equipe de Métallurgie Physique – Laboratoire des Matériaux (URA CNRS 445), Ecole Nationale Supérieure de Chimie (INPT), 118 route de Narbonne, 31077 Toulouse Cedex, France

P. COSTESEQUE, T. AIGOUY

Laboratoire de Minéralogie et Cristallographie, CRMTG (URA CNRS 67), Université Paul Sabatier, 39 allées Jules Guesde, 31000 Toulouse Cedex, France

Received 10 March 1995; revised 30 October 1995

Alumina coatings were formed by electrolytic treatment on an Fe–17% Cr stainless steel functionalized by surface conversion treatment to induce a particular surface morphology, suited to anchoring the ceramic layer. As deposited, the coatings appeared amorphous. They were composed of two layers: the superficial layer was constituted only of aluminium compounds while the deep layer had a composition gradient. Heating the coated steel caused interface reactions between the electrochemically-induced deposit and the initial conversion coating compounds. These reactions act to strengthen coat adhesion to the substrate with formation of crystallized mixed oxide such as $Fe(Cr,Al)_2O_4$. Moreover, Al_2O_3 phases appeared and acted as a barrier which prevented the thermal oxidation of the stainless steel.

1. Introduction

Ceramic films can be obtained on metallic substrates by electrochemical methods [1–12] which offer a relatively easy way to control the thickness, morphology and composition of the coat on complex shapes; the equipment is of low cost. One problem is coat adhesion at very high temperatures. In a previous paper [13] we described an original method to strengthen the interface between ceramic and substrate. This method [14] involves two steps. In the first step the substrate surface is functionalized by a conversion treatment. The conversion coating provides strong interfacial adhesion with the substrate and a particular morphology: it is very porous, with a fractal character that allows deposition during the second step and contributes to the 'anchoring' of the ceramic layer. In the second step, a refractory character is conferred to the surface by a cathodic treatment in a suitable bath which induces the deposition of oxides or hydroxides with varying degrees of hydration, giving ceramic oxides by heating in the range of 800–1000 °C depending on the alloy composition. The potential of this method for the fabrication of an alumina barrier coating on a ferritic stainless steel was demonstrated: the resistance to oxidation of the coating is high compared to that of the uncoated alloy. It is suggested that the low oxidation rate was due to an alumina barrier at the surface. The high thermal shock resistance of the coating was also demonstrated. The aim of this work is to specify the structure (morphology and chemical composition) of such alumina coatings and the transformations which occur on thermal treatment.

2. Experimental details

The deposits were prepared on an Fe–17% Cr ferritic stainless steel whose composition is given in Table 1. Specimens had dimensions of 0.6 mm × 20 mm × 50 mm. Conversion treatment was performed in a sulfuric acid solution (pH 0) with 130 ppm S^{2-}. The electrode potential of the stainless steel in the bath was controlled because one of the main conditions of the treatment is that the electrode potential fits the corrosion potential in the active state. Cathodic deposition of aluminium hydroxide [13] was performed using a platinum electrode as anode, from a saturated aqueous solution of aluminium sulfate at a potential of 3 V for 30 min. The coating analyses carried out on the substrate, in the initial state and after thermal treatment, used SIMS, X-ray diffraction and i.r. multireflection spectrometry methods. The experimental procedure for these techniques has been described elsewhere [15–17]. The microstructures were characterized using scanning electron microscopy (SEM) (Jeol model 200CX).

3. Results

3.1. *Morphology and thickness*

Visually, the conversion coating appears homogeneous and matt black. Examination by scanning

0021-891X

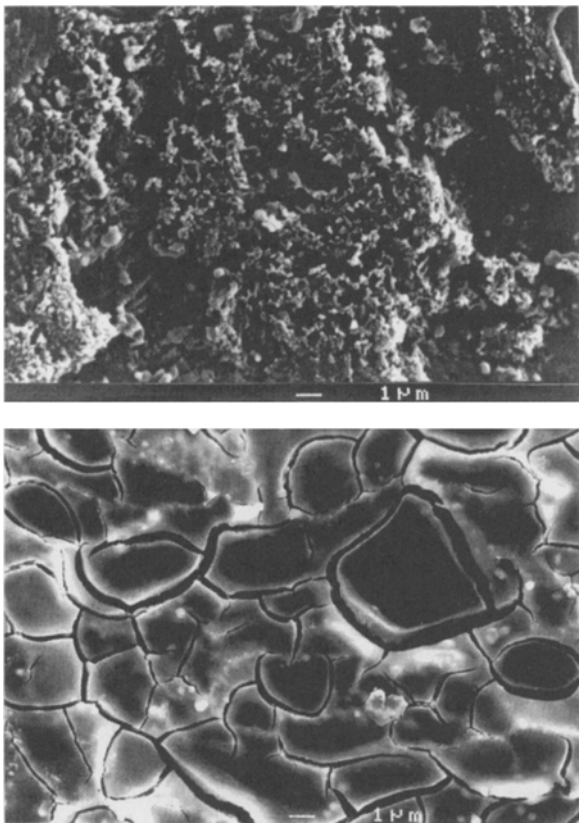

Fig. 1. SEM images of coatings: (a) initial conversion coating, and (b) final alumina deposit.

electron microscopy showed that the state of the material surface is very homogeneous and rough with pores and cavities of a large range of dimensions (Fig. 1(a)), the morphology of this adherent coating is very favourable to the anchoring of the electrolytically-induced deposit [18]. The thickness of the initial functional conversion coating, evaluated from the sputtering time by ionic bombardment (SIMS) was about 200 nm; this evaluation was made assuming that the sputtering rate did not differ with the analysed depth.

The final deposit was very uniform. Figure 1(b)

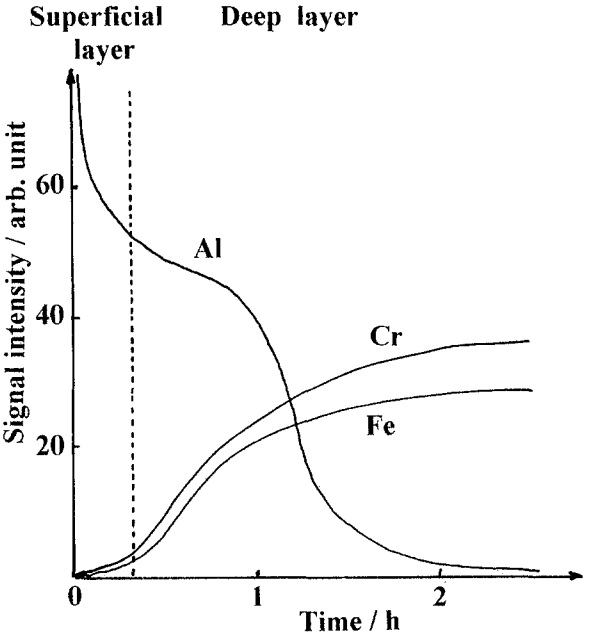

Fig. 2. Distribution profiles of the elements in the coating against bombardment time.

shows the 'cracked-mud' morphology induced on drying the wet coating whatever the substrate material. This featureless surface morphology is characteristic of the amorphous nature of the coating. Evaluation of the thickness of the deposit was not easy from sputtering time by secondary ion mass spectroscopy (SIMS). Indeed, the insulating character of the coating involves charge phenomena which hamper the ionization of species during analyses. However, by comparison with known samples, the thickness of the coat was defined as being greater than 200 nm and nearer 1 μm.

3.2. *Chemical composition*

SIMS analysis (Fig. 2) indicates that the coating was composed of two layers. (i) The deep layer corresponds to the primary conversion coating modified by the

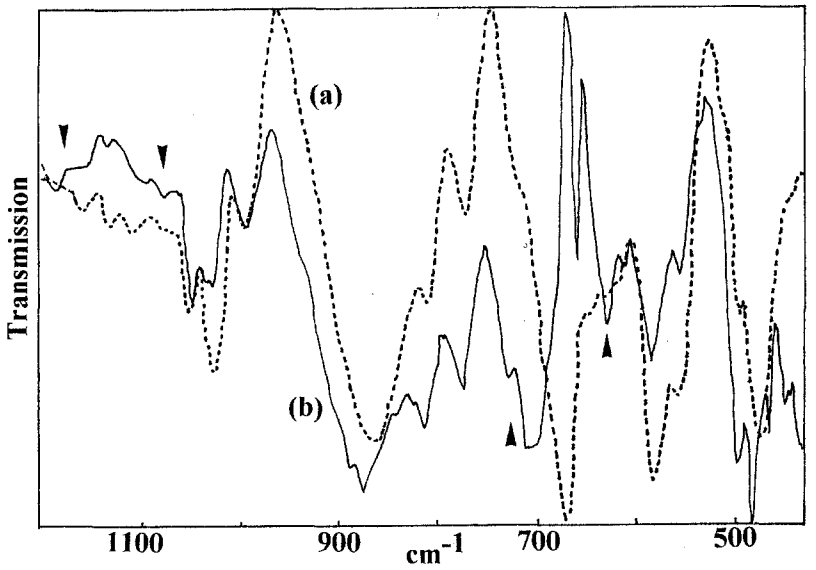

Fig. 3. Infrared multireflection spectrum of coatings: (a) initial conversion coating, and (b) coating after final alumina deposit.

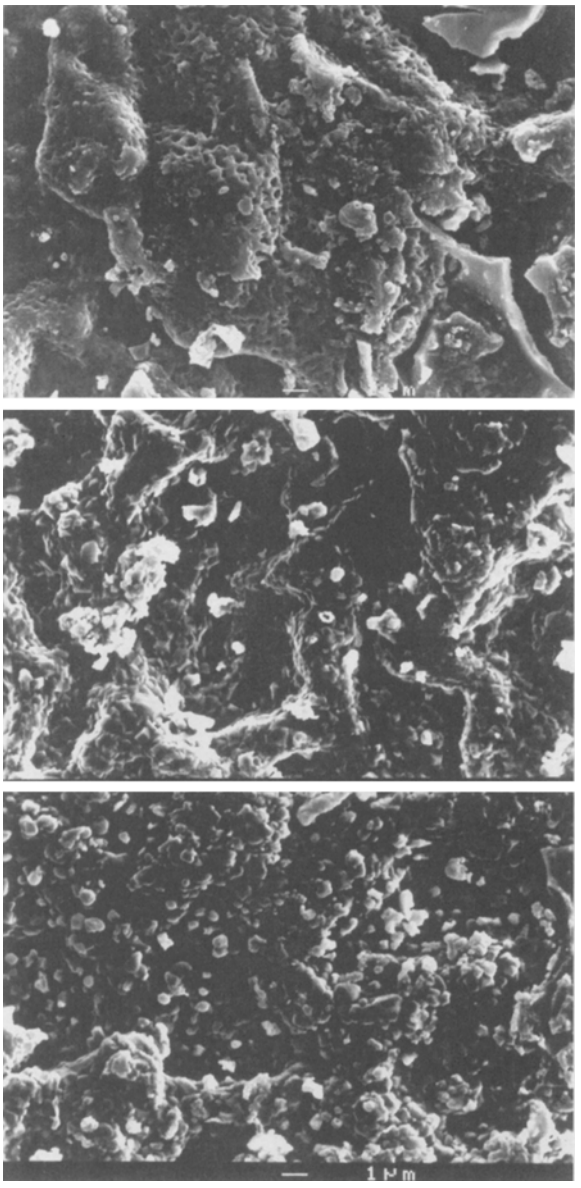

Fig. 4. SEM images of coatings after thermal treatment at various temperatures: (a) 800, (b) 900 and (c) 1000 °C.

cathodic treatment. It has composition gradients: the profiles of iron and chromium from the conversion coating were not greatly changed by the cathodic post-treatment. The aluminium profile suggests that aluminium compounds are present in the deep layer up to the stainless steel substrate. The thickness of the deep layer was that of the initial conversion coating. (ii) The superficial layer contained only aluminium compounds deposited during the cathodic treatment.

The X-ray diffraction analysis of a freshly prepared coating showed only the iron–chromium solid solution of the stainless steel substrate, so the main components which made up the coating were in the amorphous state or weakly crystallized.

Figure 3(a) shows the i.r. spectrum of the initial conversion coating essentially constituted by a chromium substituted magnetite $Fe_{3-x}Cr_xO_4$ [15, 16, 19]. Figure 3(b) shows the i.r. spectrum of the coating after final alumina deposit. The shape of this i.r. spectrum is mainly that of the substituted magnetite,

Table 1. Chemical composition of the stainless steel used (wt %)

Si	Mn	Cr	Mo	Ni	Al	Cu	Nb	Ti	Fe
0.49	0.19	15.99	0.13	0.24	0.12	0.34	0.17	0.02	Bal.

additional bands at 1160 and 1080 cm^{-1} (Al–OH vibrational mode) and at 730 and 630 cm^{-1} (Al–O vibrational mode) [20] can be attributed to aluminium oxyhydroxide AlO.OH (boehmite).

3.3. *Structural evolution during thermal treatment*

The samples were heated in air for 5 h. The initial morphology of the electrolytically-induced coating was still observed in some places after heating at 800 °C, whereas in others a very microporous structure appeared with pores of 0.5 μm. This structure may be attributed to the dehydration of the hydroxide species (Fig. 4(a)). From 900 °C, heating induced the beginning of crystallization which, at this temperature, led to the appearance of small nodules of about 0.5 μm in size (Fig. 4(b)). At 1000 °C these nodules form a compact structure over the whole surface (Fig. 4(c)).

After thermal treatment, deposits became too insulating to be studied easily by SIMS. A special thinner deposit (15 min, 3 V) was generated to represent the behaviour of the deep zone in standard deposits. The thin deposit was heated at 1000 °C. Figure 5 shows its SIMS profiles. With reference to the SIMS profiles in Fig. 2, the abrasion time of a heated coating is longer because the thermal treatment induces the compaction of the coating and the development of a harder product (Fig. 6). This indicates that the diffusion phenomena instigated by thermal treatment lead to the formation of chromium and aluminium compounds at the surface.

X-ray diffraction analysis of coatings *in situ* on the metal substrate, shows (Table 2), (Fig. 7) that:

(i) A weakly substituted hematite α-$(Fe,Cr,Al)_2O_3$ occurred at 800 °C and at 900 °C (traces); on the other hand a pure α-Fe_2O_3 phase appeared at 1000 °C.

(ii) The chromite $FeCr_2O_4$ was present at the three

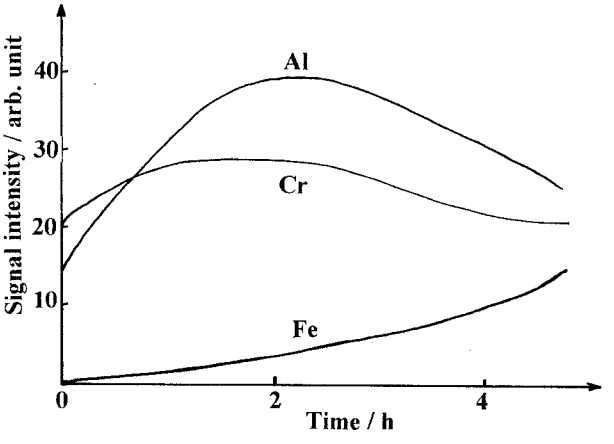

Fig. 5. Distribution profiles of the elements in the coating against bombardment time after heat treatment at 1000 °C.

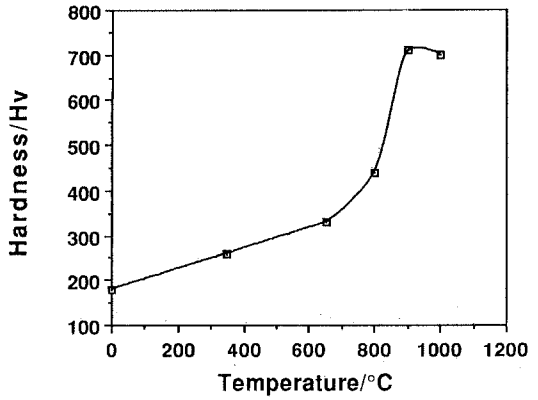

Fig. 6. Vickers microhardness of samples (using a load of 100 g) against treatment temperature.

studied temperatures with a maximum ratio at 900 °C.

(iii) The quantity of chromium oxide α-Cr_2O_3 increased from 800 °C (traces) to 1000 °C.

(iv) The substituted cubic spinel chromite $Fe(Cr,Al)_2O_4$ is observed at 900 °C and 1000 °C (the aluminium ratio, referring to the decreasing of the parameter value, particularly the diffraction peak (400) observed near 27°, probably increases with temperature).

Table 2. Phases identified in the coatings using X-ray diffraction after thermal treatments for 5 h in air at various temperatures

800 °C	900 °C	1000 °C
–	αCr_2O_3	αCr_2O_3
$[\alpha (Fe, Cr, Al)_2O_3]$	$[\alpha (Fe, Cr, Al)_2O_3]'$	–
–	–	αFe_2O_3
–	–	αAl_2O_3
$FeCr_2O_4$	$FeCr_2O_4$	$FeCr_2O_4$
–	$Fe(Cr_x, Al_{(1-x)})_2O_4$	$Fe(Cr_{x'}, Al_{(1-x')})_2O_4$

The oxides result from oxidation and/or structural modification of the primary conversion coating on thermal treatment [15, 16, 17, 21]. In particular, pure hematite may be precipitated during oxidation from iron-rich spinel solid solutions through a complex mechanism involving intermediate phase formation [22, 23]. However, the mixed oxides containing

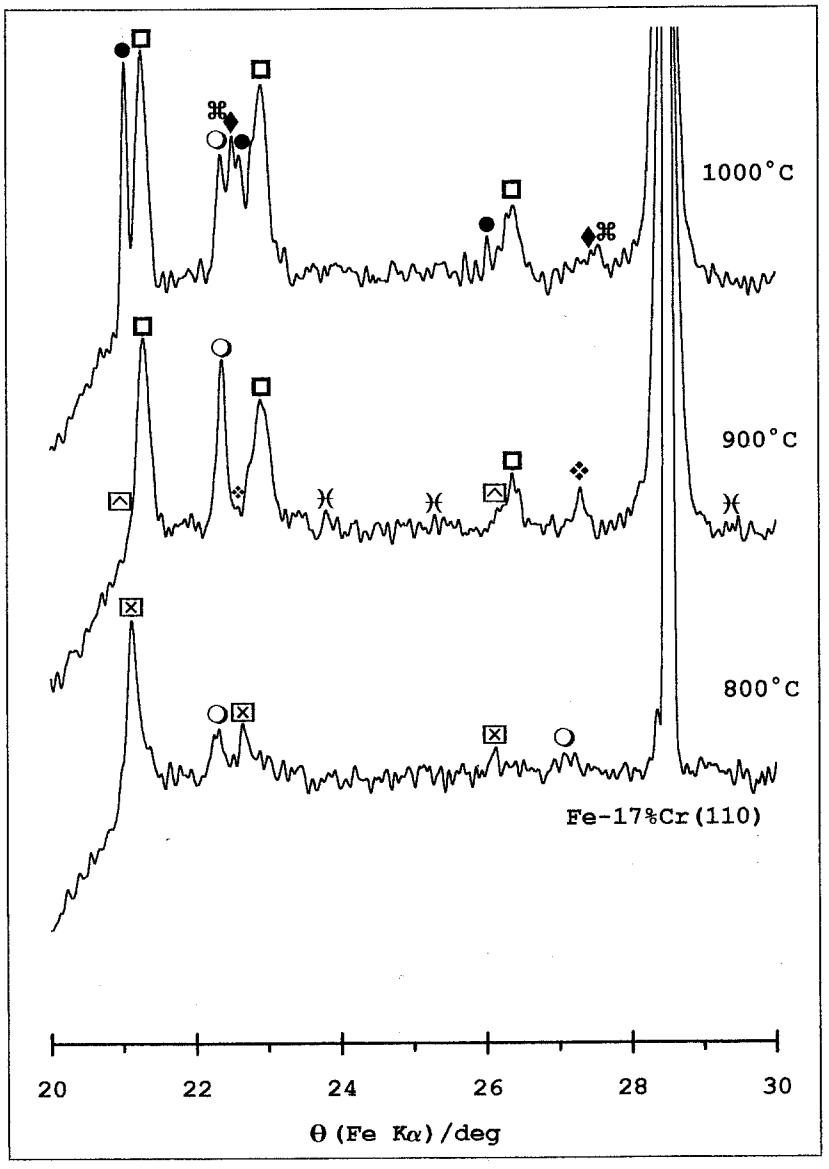

Fig. 7. X-ray diffraction spectra after heat treament at 800, 900 and 1000 °C. Legend: (□) α Cr_2O_3, (●) α Fe_2O_3, (⊠) and (⊠) weakly substituted α Fe_2O_3, (◆) and (❖) $Fe(Cr,Al)_2O_4$, (○) $FeCr_2O_4$, (⌘) α Al_2O_3, (⋕) γ Al_2O_3.

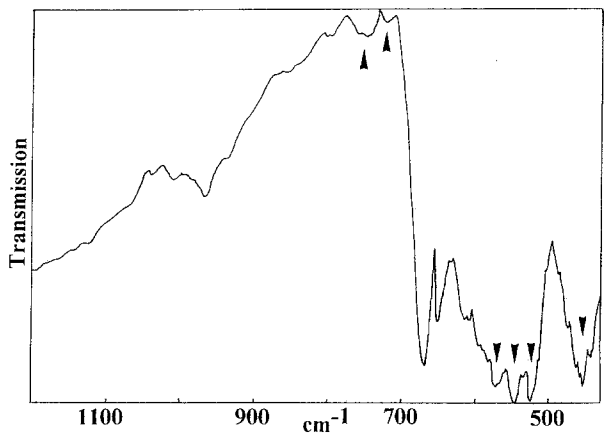

Fig. 8. Infrared multireflection spectrum of the coating after heat treatment at 1000 °C.

aluminium proceed from the reaction involving the coating compounds and the alumina deposit.

X-ray diffraction analysis (Fig. 7) shows that αAl_2O_3 clearly appears at 1000 °C, at 900 °C it also shows broad weak peaks which may be attributed to poorly crystallized γ-alumina.

Figure 8 gives the i.r. spectrum of the coating after thermal treatment in air at 1000 °C. This spectrum is different to that observed before heating; it shows a broad band in the region 800 to 400 cm^{-1} corresponding to Al–O vibrational modes. Bands at 750, 720, 575, 550–520 cm^{-1}, giving a broad absorption band between 800 and 500 cm^{-1} and associated to the very strong band at 450 cm^{-1}, are characteristic of corundum (α-Al_2O_3). The additional bands 680–660 and 620 cm^{-1} can be attributed to the $Fe(Cr,Al)_2O_4$ and αCr_2O_3 phases respectively observed by X-ray analysis.

Figure 9 shows the curves of weight change with time for the coated Fe–17% Cr alloy heated in air at 1000 °C after drying in an oven at 90 °C for 5 min. The weight loss observed from the onset of the heating and lasting 30 min corresponds to the dehydration of the coating compounds. The second phase, also of about 30 min, represents the oxidation of these compounds, essentially of the substituted magnetite which is the main component of the primary conversion coating and leads to chromite. After this second phase, the oxidation rate is very low, practically equal to zero compared to that of the bare Fe–17% Cr alloy, owing to the formation of an alumina barrier at the surface by heating the electrochemically induced aluminium oxyhydroxide.

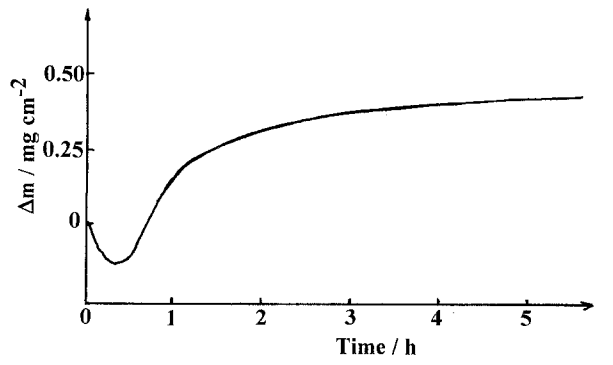

Fig. 9. Weight gain of the coating against time in air at 1000 °C.

4. Conclusion

Cathodic treatment, in an aluminium sulfate solution, of a stainless steel functionalized by a suitable conversion coating leads to the deposition of an aluminium oxyhydroxide AlO.OH boehmite. This deposition phenomenon is induced by the local rise in pH which occurs at the bottom of the pores of the conversion coating during the cathodic process. Thus, the precipitation of aluminium oxyhydroxide takes place in the conversion coating and then at its surface, the microporosity of the deposit depends on the release of hydrogen. X-ray diffraction analysis suggests that the aluminium oxyhydroxide precipitates in the amorphous state. Thus, a freshly prepared layer comprises a microporous boehmite gel. It is probable that the amorphous alumina evolves towards a partially crystalline form during the drying of the coating and with ageing; the relative proportion of coherent crystalline regions increases with time.

Thermal treatment induces consequent dehydration and modifies the structure of the boehmite gel. It is well known that the heating of boehmite in air produces a series of transition aluminas before final conversion to the thermodynamically stable corundum αAl_2O_3 [24–26]. It has been shown that the temperature at which transitions are observed is variable and that it depends, among other things, on impurities in the material [27]. In the case of this kind of electrolytically-induced deposit, some weak peaks of corundum were detected after heat treatment at 1000 °C: this temperature is lower than that commonly reported in the literature (1200 °C) for the transition temperature to the α phase probably because of the presence of other metal oxides which accelerate transformation in the deep layer.

Thermal treatment also induces interface reactions between alumina gel and conversion coating compounds with formation of chromites, which act as a bond between the substrate and the ceramic coating.

References

[1] G. E. F. Brewer, *Am. Ceram. Sci. Bull.* **51** (1972) 216.
[2] D. Tench and L. Warren, *J. Electrochem. Soc.* **130** (1983) 869.
[3] M. Sakai, T. Sekine and Y. Yamazaki, *ibid.* **130** (1983) 1631.
[4] J. A. Switzer, *ibid.* **133** (1986) 722.
[5] *Idem, Am. Ceram. Soc. Bull.* **66** (1987) 1521.
[6] H. Konno, *J. Electrochem. Soc.* **134**(4) (1987) 1034.
[7] H. Konno and R. Furuichi, *J. Met. Finish. Soc. Japan* **39**(1) (1988) 29.
[8] H. Konno, M. Tokita and R. Furuichi, *J. Electrochem. Soc.* **137**(1) (1990) 361.
[9] L. Gal-or, I. Silberman and R. Chaim, *ibid.* **138**(7) (1991) 1939.
[10] R. Chaim, I. Silberman and L. Gal-or, *ibid.* **138**(7) (1991) 1942.
[11] G. Aguilar, J. C. Colson and J. P. Larpin, *Mem. Sci. Rev. Met.* **7–8** (1992) 447.

[12] H. Konno, M. Tokita, A. Furusaki and R. Furuichi, *Electrochim. Acta* **37**(13) (1992) 2421.
[13] L. Aries, *J. Appl. Electrochem.* **24** (1994) 554.
[14] L. Aries and F. Dabosi, *Brevet INPT 9 312 790.*
[15] L. Aries, J. Roy, T. Bouissou and R. Sempere, *Mater. Sci. Technol.* **7** (1991) 24.
[16] L. Aries, J. Roy, B. Naboulsi, T. Bouissou and R. Sempere, *Mater. Sci. Technol.* **7** (1991) 757.
[17] L. Aries, M. El Bakkouri, J. Roy, J.P. Traverse, R. Calsou and R. Sempere, *Thin Solid Films* **197** (1991) 143.
[18] M. M. Hefny, *J. Appl. Electrochem.* **21** (1991) 485.
[19] B. Gillot, F. Bouton, F. Chassagneux and A. Rousset, *J. Solid State Chem.* **33** (1980) 245.
[20] V. Sarawasti, G. V. N. Rao and G. V. Rama Rao, *J. Mater. Sci.* **22** (1987) 2529.
[21] S. C. Tjong, *Werkst. Korros.* **37** (1986) 591.
[22] T. Yamaguchi and T. Kimura, *J. Am. Ceram. Soc.* **59**(7–8) (1976) 333.
[23] T. Kimura, S. Ohishi and T. Yamaguchi, *J. Am. Ceram. Soc.* **228**(7) (1979) 533.
[24] Rong-Sheng Zhou and R. L. Snyder, *Acta. Cryst.* **B47** (1991) 617.
[25] J. E. Bonevich and L. D. Marks, *J. Mater. Res.* **7** (1992) 1489.
[26] A. Tonejc, M. Stubicar, A. M. Tonejc, K. Kosanovic, B. Subotic and I. Smit, *J. Mater. Sci. Lett.* **13** (1994) 519.
[27] L. Pach, R. Roy and S. Komarneni, *J. Mater. Res.* **5** (1990) 278.